The chromodomain protein, Chromator, interacts with JIL-1 kinase and regulates the structure of *Drosophila* polytene chromosomes

Uttama Rath*, Yun Ding*, Huai Deng, Hongying Qi, Xiaomin Bao, Weiguo Zhang, Jack Girton, Jørgen Johansen and Kristen M. Johansen‡

Department of Biochemistry, Biophysics, and Molecular Biology, Iowa State University, Ames, Iowa 50011, USA

*These authors contributed equally to this work

‡Author for correspondence (e-mail: kristen@iastate.edu)

Accepted 24 February 2006

Journal of Cell Science 119, 2332-2341 Published by The Company of Biologists 2006

doi:10.1242/jcs.02960

Summary

In this study we have generated two new hypomorphic *Chro* alleles and analyzed the consequences of reduced Chromator protein function on polytene chromosome structure. We show that in $Chro^{71}/Chro^{612}$ mutants the polytene chromosome arms were coiled and compacted with a disruption and misalignment of band and interband regions and with numerous ectopic contacts connecting non-homologous regions. Furthermore, we demonstrate that Chromator co-localizes with the JIL-1 kinase at polytene interband regions and that the two proteins interact within the same protein complex. That both proteins are necessary and may function together is supported by the finding that a concomitant reduction in JIL-1 and Chromator function synergistically reduces viability during development. Overlay assays and deletion construct analysis suggested that the interaction between JIL-1 and Chromator is direct and that it is mediated by sequences in the C-terminal domain of Chromator and by the acidic region within the C-terminal domain of JIL-1. Taken together these findings indicate that Chromator and JIL-1 interact in an interband-specific complex that functions to establish or maintain polytene chromosome structure in *Drosophila*.

Key words: JIL-1 kinase, Chromodomain, Chromator, Chromatin structure, *Drosophila*

Introduction

A striking feature of *Drosophila* polytene chromosomes is the stable and reproducible organization of chromatin into band and interband regions (Zhimulev, 1996). Interband regions are made up of parallel-oriented 10 nm chromosome fibrils loosely aligned whereas in banded regions the chromatin is further compacted into 30 nm fibrils forming higher-order loops or toroidal structures, the exact nature of which is still ill-defined (Mortin and Sedat, 1982; Ananiev and Barsky, 1985; Schwartz et al., 2001; Zhimulev et al., 2004). It is generally thought that this difference in chromatin organization correlates with important aspects of how gene expression is regulated (Zhimulev and Belyaeva, 2003). However, little is known about the molecules and molecular mechanisms that are responsible for controlling the establishment and maintenance of polytene chromatin morphology. With the goal of identifying such molecules we have recently characterized a new tandem kinase in *Drosophila*, JIL-1, that localizes specifically to euchromatic interband regions of polytene chromosomes (Jin et al., 1999) and which is the predominant kinase regulating histone H3S10 phosphorylation at interphase (Wang et al., 2001). Analysis of *JIL-1* null and hypomorphic alleles showed that *JIL-1* is essential for viability and that reduced levels of JIL-1 protein lead to a misalignment of the interband polytene chromatin fibrils that is further associated with coiling of the chromosomes and an increase of ectopic contacts between non-homologous regions. (Jin et al., 2000; Wang et al., 2001; Zhang et al., 2003; Deng et al., 2005). This results in a shortening and folding of the chromosomes with a non-orderly intermixing of euchromatin and the compacted chromatin characteristic of banded regions (Deng et al., 2005). The intermingling of non-homologous regions can be so extensive that these regions become fused and confluent, further shortening the chromosome arms. Based on these findings a model was proposed where JIL-1 functions to establish or maintain the parallel alignment of interband chromosome fibrils as well as to repress the formation of contacts and intermingling of non-homologous chromatid regions (Deng et al., 2005).

Another protein that localizes specifically to interband regions of polytene chromosomes is the chromodomain protein, Chromator (Rath et al., 2004). Chromator was originally identified in a yeast two-hybrid screen as an interaction partner of the putative spindle matrix component, skeletor, and localizes to the spindle and the centrosomes during mitosis (Rath et al., 2004). Furthermore, functional assays using RNAi-mediated depletion in S2 cells suggest that Chromator directly affects spindle function and chromosome segregation (Rath et al., 2004). However, localization of Chromator to polytene interbands suggests it also has a functional role in maintaining chromatin structure during interphase. Such a role is supported by the finding of Eggert et al. (Eggert et al., 2004) that Chromator (which these workers refer to as Chriz) is found in a protein complex together with the interband-specific zinc-finger protein Z4 (Eggert et al.,

2004; Gortchakov et al., 2005). That Z4 participates in regulating polytene chromosomal structure is likely because *Z4*-null mutant chromosomes show a decompaction of chromatin and a loss of a clear band/interband pattern (Eggert et al., 2004). However, the effect of Chromator on polytene chromosome morphology has been difficult to study because null alleles of *Chro* die as embryos or first-instar larvae before salivary gland polytene chromosomes can be analyzed (Rath et al., 2004; Gortchakov et al., 2005). For this reason we performed an EMS mutagenesis screen that generated two new *Chro* hypomorphic alleles. The analysis of these alleles shows that impaired Chromator function leads to disorganization and misalignment of band/interband regions resulting in coiling and folding of the polytene chromosomes. In addition, we demonstrate that Chromator directly interacts with JIL-1 kinase and that the two proteins extensively co-localize at polytene interband regions. Taken together these findings indicate that Chromator and JIL-1 interact in an interband-specific complex that functions to establish or maintain polytene chromosome structure in *Drosophila*.

Results

Chromator and JIL-1 kinase directly interact

The interphase localization of Chromator to polytene chromosome interband regions (Rath et al., 2004; Eggert et al., 2004; Gortchakov et al., 2005) is very similar to that reported for the JIL-1 histone H3S10 kinase (Jin et al., 1999; Jin et al., 2000; Wang et al., 2001). For this reason we explored whether the two proteins were present in the same macromolecular complex by performing co-immunolocalization and biochemical studies. Fig. 1 shows confocal images of a double labeling with JIL-1- and Chromator-specific antibodies of a third-instar larval polytene chromosome squash preparation. JIL-1 localization is shown in green, Chromator protein localization in red, and co-localization is indicated by yellow regions in the composite image. The predominantly yellow labeling in the composite image indicates that JIL-1 co-localizes with Chromator extensively along the entire length of the chromosome arms (Fig. 1A). At some band locations in the composite image the color is more green or orange than pure yellow as a result of slight differences in the relative staining intensity of the two antibodies, which can vary from preparation to preparation. However, in all cases examined the banding patterns themselves appeared identical (Fig. 1B,C) providing evidence that Chromator and JIL-1 are co-localized at most if not all interband regions.

In order to probe further for a potential interaction we performed immunoprecipitation (IP) experiments using S2 cell lysates. For these experiments, proteins were extracted from S2 cells, immunoprecipitated using either JIL-1- or Chromator-specific antibodies, fractionated on SDS-PAGE after the IP, immunoblotted, and probed with antibodies to Chromator and JIL-1, respectively. Fig. 2A shows an IP experiment using an anti-Chromator antibody where the immunoprecipitate is detected by JIL-1 antibody as a 160 kDa band that is also present in the S2 cell lysate. This band was not present in the lane where only immunobeads were used for the IP (Fig. 2A). Fig. 2B shows the converse experiment: JIL-1 antiserum immunoprecipitated a 130 kDa band detected by Chromator antibody that was also present in S2 cell lysate but not in control IPs with immunobeads only. Furthermore, we stably and transiently transfected S2 cells with a V5-tagged full-length Chromator contruct and prepared nuclear extracts from lysed cells. Fig. 2C shows an IP experiment using V5 antibody where a 160 kDa band detected by the anti-JIL-1 antibody that was also present in the S2 cell nuclear extract was co-immunoprecipitated. This band was not present in the lane where the V5 antibody IP was performed in nuclear extracts from untransfected control S2 cells (Fig. 2C). These results strongly indicate that Chromator and the JIL-1 kinase are present in the same protein complex.

To characterize further the interaction between Chromator and JIL-1 and to identify the domains mediating the interaction we performed overlay assays with GST-fusions of various regions of the two proteins. For the initial screening of JIL-1 we used four GST-fusion proteins covering the N-terminal domain (JIL-1-NTD), the first kinase domain (JIL-1-KDI), the second kinase domain (JIL-1-KDII), and the C-terminal domain (JIL-1-CTD) as illustrated in Fig. 3A. For Chromator we generated an N-terminal construct including the chromodomain (Chro-NTD) as well as a C-terminal construct (Chro-CTD) (Fig. 3A). Fig. 3B,C shows JIL-1 GST-fusion proteins that were coupled with glutathione agarose beads, washed, fractionated by SDS-PAGE, transferred to nitrocellulose paper, and incubated with glutathione-agarose-bead-purified Chro-CTD and Chro-NTD GST-fusion constructs, respectively. Protein interactions were detected with Chromator C-terminal mAb 6H11 in Fig. 3B and with the N-terminal Chromator mAb 12H9 in Fig. 3C. As illustrated in Fig. 3B (arrows) only the JIL-1-CTD and Chro-CTD fusion constructs were found to interact in these assays. Western blot analysis of the GST proteins purified in these experiments and detected with anti-GST antibody showed that similar levels of JIL-1-NTD, JIL-1-KDI, JIL-1-KDII and JIL-1-CTD fusion proteins were present in these assays (Fig. 3D). Immunoblots of the purified Chro-CTD and Chro-NTD fusion constructs used for the overlays are shown in Fig. 3B (lane 6) and Fig. 3C (lane 7), respectively. The region of JIL-1 that was found

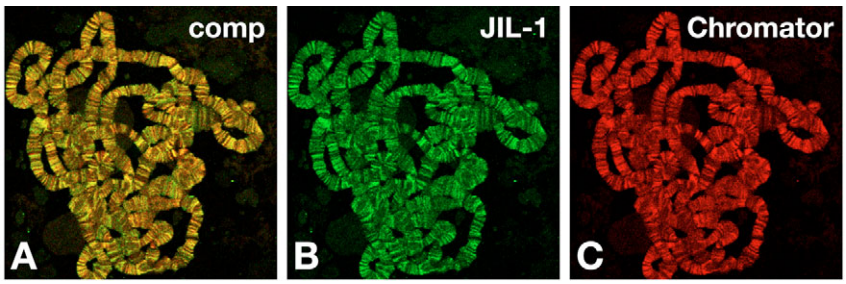

Fig. 1. Co-localization of JIL-1 with Chromator at polytene chromosome bands. Double labeling of a female polytene chromosome squash preparation with antibodies against JIL-1 (B) and Chromator (C). The composite image (A) shows the extensive overlap between JIL-1 (green) and Chromator (red) labeling at a large number of chromosome bands as indicated by the predominantly yellow color. The images are from confocal sections.

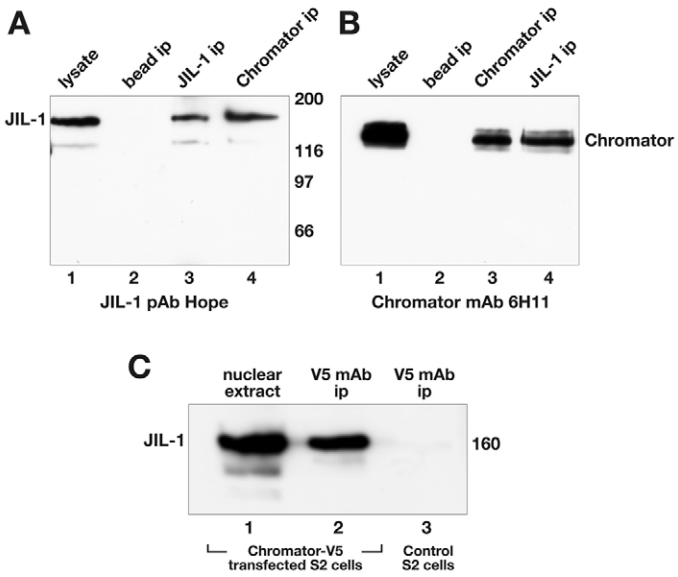

Fig. 2. Chromator and JIL-1 immunoprecipitation assays.
(A) Immunoprecipitations (ip) of lysates from S2 cells were performed using Chromator antibody (mAb 6H11, lane 4) and JIL-1 antibody (Hope antiserum, lane 3) coupled to immunobeads or with immunobeads only as a control (lane 2). The immunoprecipitations were analyzed by SDS-PAGE and western blotting using JIL-1 pAb for detection. JIL-1 antibody staining of S2 cell lysate is shown in lane 1. JIL-1 is detected in the JIL-1 and Chromator immunoprecipitation samples as a 160 kDa band (lane 3 and 4, respectively) but not in the control sample (lane 2).
(B) Immunoprecipitations of lysates from S2 cells were performed using Chromator antibody (mAb 6H11, lane 3) and JIL-1 antibody (Hope antiserum, lane 4) coupled to immunobeads or with immunobeads only as a control (lane 2). The immunoprecipitations were analyzed by SDS-PAGE and western blotting using Chromator mAb 6H11 for detection. Chromator antibody staining of S2 cell lysate is shown in lane 1. Chromator is detected in the JIL-1 and Chromator immunoprecipitation samples as a 130 kDa band (lane 4 and 3, respectively) but not in the control sample (lane 2). The relative migration of molecular size markers are indicated in kDa.
(C) Immunoprecipitations of nuclear extracts from S2 cells were performed using V5 antibody from cells transfected with a V5-tagged full-length Chromator (lane 2) or from untransfected cells as a control (lane 3). The immunoprecipitations were analyzed by SDS-PAGE and western blotting using JIL-1 antiserum for detection. JIL-1 antibody staining of S2 cell nuclear extract is shown in lane 1. JIL-I is detected as a 160 kDa band in V5-antibody immunoprecipitates from V5-tagged Chromator transfected S2 cells (lane 2) but not in the untransfected control samples (lane 3).

to interact with Chromator, the JIL-1 CTD-domain, can be further divided into two distinct regions (Bao et al., 2005): an acidic region from residues 887-1033 that has a predicted pI <4 and a basic region from residues 1034-1207 that has a pI >11 (Fig. 3A). Thus, in order to define the sequences of JIL-1 responsible for the molecular interaction between JIL-1 and Chromator, we generated GST fusion proteins comprising these two regions, JIL-1-CTD-A and JIL-1-CTD-B (Fig. 3A), and performed overlay experiments with the Chro-CTD construct as described above. As shown in Fig. 3E the JIL-1-CTD and JIL-1-CTD-A fusion proteins both interacted with Chro-CTD as detected by Chromator mAb 6H11 (arrows) whereas JIL-1-CTD-B or GST alone did not. Western blot analysis of the GST proteins purified in these experiments and detected with GST-antibody showed that approximately equivalent levels of JIL-1-CTD, JIL-1-CTD-A, and JIL-1-CTD-B fusion proteins were present in these assays (Fig. 3F). An immunoblot of the purified Chro-CTD fusion construct used for the overlay is shown in Fig. 3E (lane 5). Taken together these results suggest that the interaction between JIL-1 and Chromator is direct and that it is mediated by sequences in the C-terminal domain of Chromator and by the acidic region within the C-terminal domain of JIL-1.

Generation of hypomorphic Chromator alleles

We have previously demonstrated that the P-element insertion *KG03258* is a lethal loss-of-function mutation in the *Chro* gene (Rath et al., 2004). Unfortunately, most homozygous *KG03258* animals die as embryos and none survive past the first-instar larval stages, thus precluding the analysis of polytene chromosome structure in third-instar larval salivary gland cells. Attempts to generate new hypomorphic loss-of-function *Chro* alleles that survive to third-instar larval stages by imprecise P-element excisions have so far been unsuccessful (Rath et al., 2004; Gortchakov et al., 2005). In addition, such studies are likely to be complicated by the close proximity of the essential neighboring *ssl1* gene to the *Chro* locus (Rath et al., 2004; Gortchakov et al., 2005). For these reasons we generated EMS-induced point mutations in the *Chro* gene using standard protocols (Grigliatti, 1986). We identified a total of 12 new alleles that reduced adult survival rates by more than 50% when heterozygous with the *KG03258* allele compared with a wild-type allele. Complementation tests between the newly generated alleles revealed that individuals heteroallelic for two of these alleles survive to third-instar larval stages. These two alleles were subsequently sequenced and further characterized in this study. The $Chro^{71}$ allele is comprised of a G to A nucleotide change at nucleotide position 402 of the *Chro* coding sequence that introduces a premature stop codon resulting in a truncated 71 amino acid protein (Fig. 4A). The truncated N-terminal fragment does not contain the chromodomain and $Chro^{71}$ probably acts as a strong hypomorphic or null allele. $Chro^{71}$ is homozygous embryonic lethal with no first-instar larval escapers. The $Chro^{612}$ allele consists of a C to T nucleotide change at nucleotide position 2024 that introduces a premature stop codon resulting in a truncated 612 amino acid protein that retains the chromodomain (Fig. 4A). $Chro^{612}$ is homozygous embryonic lethal with a few first-instar larval escapers. However, $Chro^{71}/Chro^{612}$ transheterozygotes survived to third-instar larval stages although no larvae have been observed to pupate. This suggests that $Chro^{612}$ is a severe hypomorphic loss-of-function allele that nonetheless in combination with $Chro^{71}$ can provide partial function sufficient for development to third-instar stages. Although genetic crosses were performed to replace the other chromosomes it should be noted that the presence of second site mutations on the third chromosome cannot be ruled out and may account for the early lethality of homozygous $Chro^{612}$ mutants. However, the effect of such potential mutations are probably masked in the $Chro^{71}/Chro^{612}$ transheterozygotes. The immunoblot of protein extracts from wild-type and $Chro^{71}/Chro^{612}$ third-instar larvae in Fig. 4B

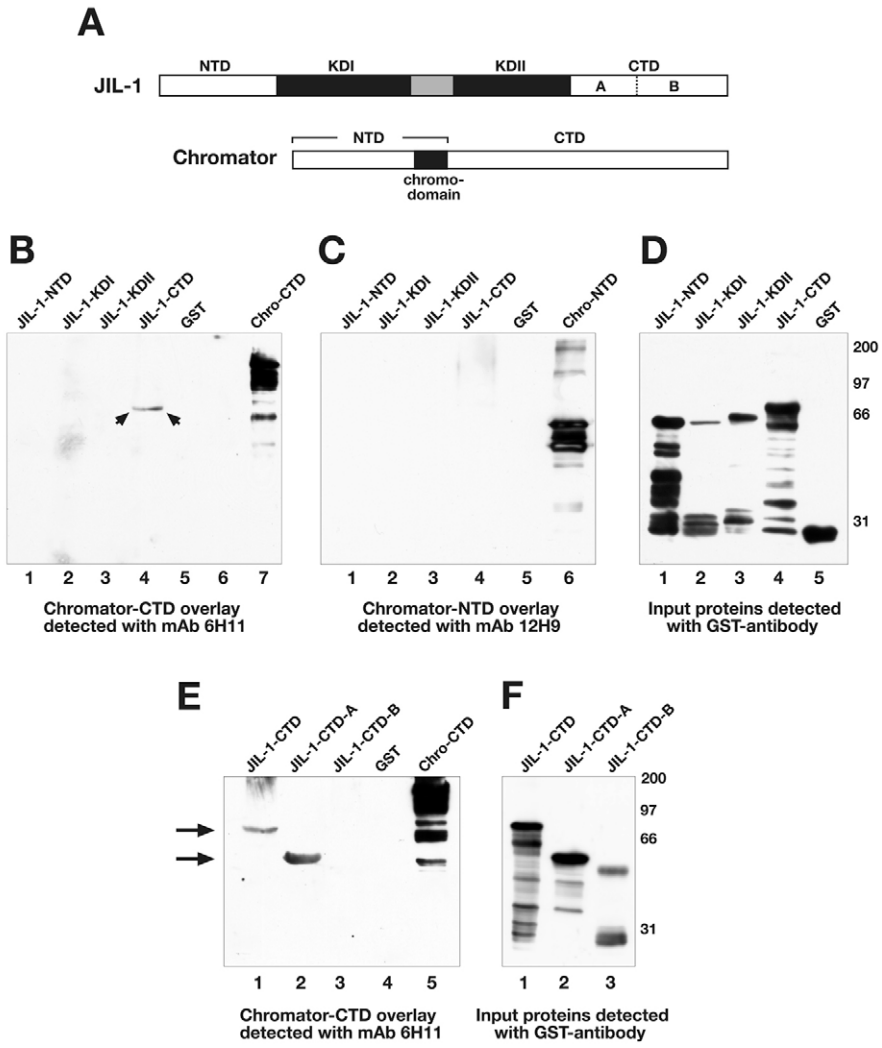

Fig. 3. Mapping of the JIL-1 interaction domain with Chromator. (A) Diagrams of the JIL-1 and Chromator proteins indicating the domains to which GST-fusion proteins were made for mapping. In the overlay experiments various truncated JIL-1 GST-fusion protein constructs to the domains in A or a GST-only control were fractionated by SDS-PAGE, western blotted, incubated with Chro-CTD (B) or Chro-NTD (C) GST-fusion protein, and interactions detected with the C-terminal Chromator mAb 6H11 (B) or the N-terminal Chromator mAb 12H9 (C). The only interaction detected was between the JIL-1-CTD and Chro-CTD fusion proteins (arrows in B). Immunoblots of the overlay GST-fusion proteins Chro-CTD and Chro-NTD are shown (B, lane 7 and C, lane 6, respectively). (D) Immunoblot of the input GST-fusion proteins used for the overlay experiments in B and C detected with the anti-GST mAb 8C7. (E) Overlay experiments with truncated C-terminal JIL-1 GST-fusion protein constructs to the subdomains shown in A or a GST-only control were fractionated by SDS-PAGE, western blotted, incubated with Chro-CTD, and interactions detected with the C-terminal Chromator mAb 6H11. In these experiments interactions between Chro-CTD and JIL-1-CTD as well as JIL-1-CTD-A were detected (arrows) but not between Chro-CTD and JIL-1-CTD-B. An immunoblot of the overlay GST-fusion protein Chro-CTD is shown in lane 5. (F) Immunoblot of the input GST-fusion proteins used for the overlay experiments in E detected with the anti-GST mAb 8C7. This defined the JIL-1 C-terminal acidic domain as sufficient for mediating interactions with the C-terminal domain of Chromator. The relative migration of molecular size markers is indicated to the right of the immunoblots in kDa.

demonstrates that no detectable full-length Chromator protein was present in the mutant larvae. The immunoblot was labeled with Chromator-specific mAb 6H11 (Rath et al., 2004) which was generated to C-terminal sequence deleted in both the *Chro*^{71} and *Chro*^{612} alleles.

Polytene chromosome structure is disrupted in hypomorphic Chromator mutants

The generation of severely hypomorphic *Chro* alleles that as transheterozygotes survived to third-instar larval stages allowed the analysis of their effect on polytene chromosome structure. Fig. 4C,D shows a comparison of polytene squashes from wild-type and *Chro*^{71}/*Chro*^{612} larvae labeled with Hoechst 33258 stain. Whereas wild-type polytene chromosomes show extended arms with a regular pattern of Hoechst-stained bands (Fig. 4C), this pattern is severely perturbed in *Chro*^{71}/*Chro*^{612} mutant larvae (Fig. 4D). In the latter preparations band/interband regions were disrupted and the chromosome arms were coiled and condensed (Fig. 4D). To understand the underlying causes of these defects we performed an ultrastructural analysis by preparing squashes of polytene chromosomes from *Chro*^{71}/*Chro*^{612} third-instar larvae for transmission electron microscopy (TEM) and comparing them with squashes from wild-type larvae (Fig. 5). Fig. 5A shows the orderly segregation into interband and the more electron-dense banded regions in TEM of a wild-type autosome. However, in *Chro*^{71}/*Chro*^{612} mutants the alignment of the chromatids in the interbands was disrupted and the orderly arrangement of compacted chromatin in the banded regions was severely affected as well (Fig. 5B,C). Another feature of the phenotype was the folding and coiling of the chromosomes with numerous ectopic contacts connecting non-homologous regions (Fig. 5C). However, despite these disruptions, distinct band and interband regions were still clearly discernable in the mutant chromosomes. These findings suggest that normal Chromator function is required for maintaining the orderly segregation of bands and interbands in polytene chromosome structure.

Localization of Chromator and JIL-1 in mutant polytene chromosomes

The finding that Chromator and JIL-1 directly interact within the same protein complex raised the question whether one of the proteins is required for the polytene chromosome localization of the other. To address this issue we performed double labelings of polytene squashes from wild-type,

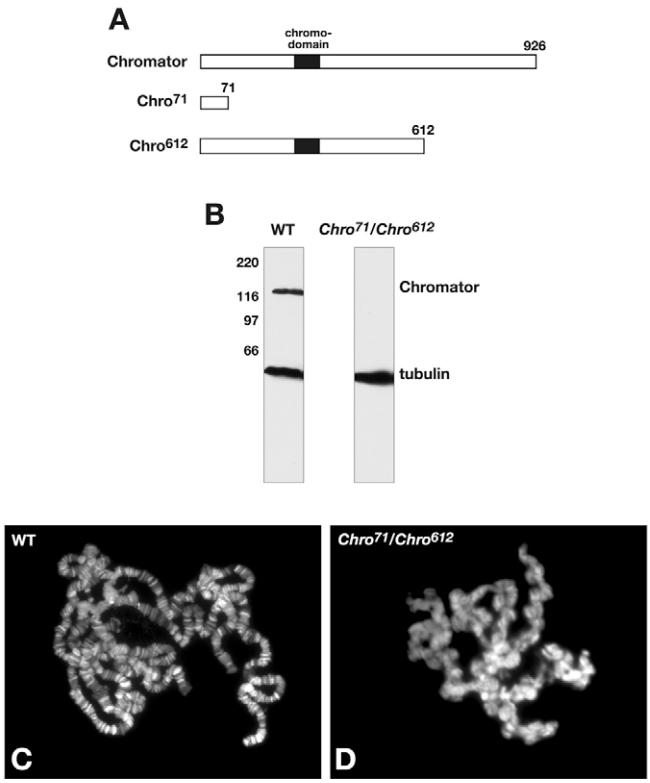

Fig. 4. EMS induced *Chro* alleles. (A) Diagram of the wild-type Chromator protein and the potential truncated protein products of the EMS induced *Chro* alleles, $Chro^{71}$ and $Chro^{612}$. The $Chro^{71}$ allele is comprised of a G to A nucleotide change at nucleotide position 402 of the *Chro* coding sequence that introduces a premature stop codon resulting in a truncated 71 amino acid protein. The $Chro^{612}$ allele consists of a C to T nucleotide change at nucleotide position 2024 that introduces a premature stop codon resulting in a truncated 612 amino acid protein that retains the chromodomain. (B) Chromator protein expression in $Chro^{71}/Chro^{612}$ mutant third-instar larvae compared with wild type larvae. The immunoblots were labeled with the C-terminal Chromator mAb 6H11 and with anti-tubulin antibody as a loading control. Full-length Chromator is detected as a 130 kDa protein by mAb 6H11 in wild-type larvae; however, no full-length Chromator is detectable in the mutant larvae. The relative migration of molecular weight markers is indicated to the left of the immunoblots in kDa. (C,D) Polytene chromosome preparations from third-instar larvae were labeled with Hoechst to visualize the chromatin. Preparations are shown from a wild-type female larvae (C) and from a female $Chro^{71}/Chro^{612}$ mutant larvae (D). Reduced levels of wild-type Chromator protein have a severe effect on the structure and organization of larval polytene chromosomes. Note the disruption and misalignment of interband and banded regions and the extensive coiling and folding of the chromosome arms in $Chro^{71}/Chro^{612}$ mutant chromosomes (D).

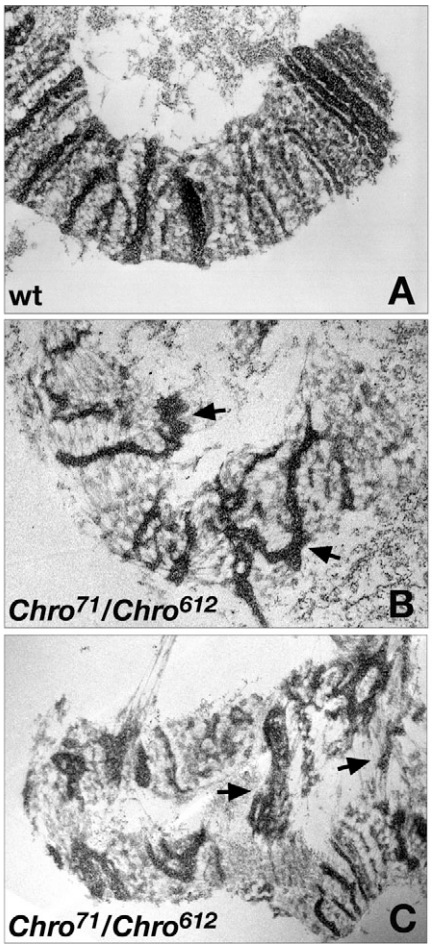

Fig. 5. Ultrastructure of $Chro^{71}/Chro^{612}$ mutant polytene chromosomes. (A) TEM micrograph of a wild-type polytene chromosome. Note the clear segregation into bands and interbands and the orderly alignment of euchromatic chromatid fibrils. (B,C) Chromosomes from $Chro^{71}/Chro^{612}$ polytene salivary gland nuclei. The micrograph in B shows the disorganization and misalignment of band/interband polytene chromosome regions (arrows). The micrograph in C shows the folding and coiling of the chromosomes with numerous ectopic contacts connecting non-homologous regions (arrows).

$Chro^{71}/Chro^{612}$, and $JIL\text{-}1^{z2}/JIL\text{-}1^{z2}$ third-instar larvae with the JIL-1 pAb Hope and the Chromator mAb 6H11. The $JIL\text{-}1^{z2}$ allele is a true null that when homozygous produces no JIL-1 protein (Wang et al., 2001; Zhang et al., 2003). Banded regions of the polytene chromosomes were labeled with Hoechst 33258. Fig. 6A (upper panel) shows that in wild-type polytene squashes both Chromator and JIL-1 colocalize to interband regions in a pattern complementary to the Hoechst labeling. In $Chro^{71}/Chro^{612}$ mutants the polytene chromosome morphology is perturbed; however, JIL-1 continued to be localized to interband regions not labeled by Hoechst (Fig. 6A, middle panel). No full-length Chromator protein was detected by mAb 6H11, which recognizes a C-terminal epitope (Rath et al., 2004) in these preparations. In the *JIL-1* null mutants with no detectable JIL-1 protein the chromosome morphology was also severely perturbed as previously described (Wang et al., 2001; Deng et al., 2005); nonetheless, Chromator still localized to chromosome regions in a complementary pattern to the Hoechst labeling of compacted chromatin (Fig. 6A, bottom panel). These data strongly suggest that Chromator localization to the polytene chromosomes does not depend on the JIL-1 protein. However, JIL-1 dependence on the Chromator protein could not be ruled out by these experiments because the $Chro^{612}$ allele can give rise to a truncated Chromator protein

that contains the chromodomain and that has enough C-terminal sequence to potentially recruit JIL-1. The *Chro*^{71} allele is unlikely to play such a role because it lacks the entire C-terminal domain and because the N-terminal region of Chromator is without a functional nuclear localization signal (Rath et al., 2004). Labelings of *Chro*^{71}/*Chro*^{612} mutant polytene squashes with the N-terminal Chromator mAb 12H9 showed that Chro^{612} protein indeed localizes to the interband regions of the polytene chromosomes (Fig. 6B). We therefore used RNAi methods in S2 cells to completely deplete Chromator levels and assayed for the consequences on JIL-1 localization by labeling with JIL-1 antibody. In control cells, as shown in Fig. 7 JIL-1 antibody specifically labels the chromatin and is upregulated on the X chromosome (the S2 cell line is a 'male' cell line) as previously described (Jin et al., 1999; Jin et al., 2000; Wang et al., 2001). To verify that it was indeed the X chromosome that had upregulated JIL-1 levels the preparations were double labeled with anti-MSL-1 antibody. MSL-1 is a member of the MSL (male-specific lethal) dosage compensation complex and is found only on the male X chromosome (Kuroda et al., 1991; Kelley and Kuroda, 1995). However, the distribution of JIL-1 did not change in *Chro* RNAi-treated cell cultures (Fig. 7A, bottom panel) where Chromator protein levels were reduced below limits detectable by immunoblot analysis (Fig. 7B). These results suggest that Chromator is not required for JIL-1 localization to chromatin nor for upregulation of JIL-1 on the male X chromosome. Similar results were also obtained for male *Chro*^{71}/*Chro*^{612} mutant polytene chromosomes labeled with JIL-1 antibody (Fig. 6C). Furthermore, although the phenotype of *JIL-1* and *Chro*^{71}/*Chro*^{612} mutant polytene chromosomes generally resemble each other, a notable difference is that the morphology of the male X chromosome in *Chro*^{71}/*Chro*^{612} larvae was similar to that of the autosomes (Fig. 6C) and not 'puffed' as in *JIL-1* null mutants (Wang et al., 2001; Deng et al., 2005). Although these experiments indicate that Chromator does not directly recruit JIL-1 to polytene chromosomes the presence of truncated Chromator proteins in the *Chro*^{71}/*Chro*^{612} mutant does not allow us to completely exclude the possibility of an indirect requirement.

Genetic interactions between *Chro* and *JIL-1* alleles

To determine whether Chromator and JIL-1 genetically interact in vivo we explored interactions between mutant alleles of

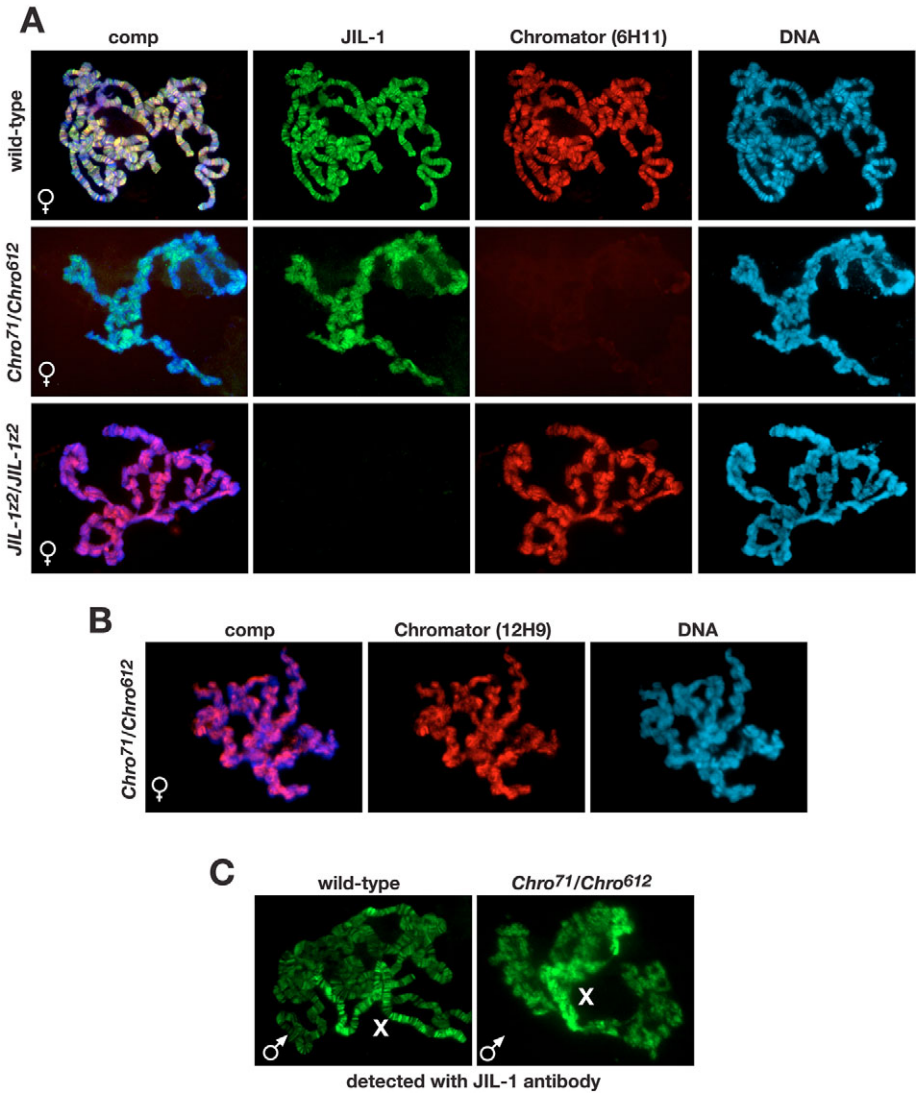

Fig. 6. Localization of JIL-1 and Chromator in mutant polytene chromosomes. (A) Triple labelings with the JIL-1 pAb Hope (green), the C-terminal Chromator mAb 6H11 (red) and Hoechst 33258 (blue) of polytene squashes from wild-type (upper panel), *Chro*^{71}/*Chro*^{612} (middle panel), and *JIL-1*^{z2}/*JIL-1*^{z2} (lower panel) female third-instar larvae. The composite image (comp) is shown to the left. The mAb 6H11 epitope is not present in either of the truncated Chro^{71} or Chro^{612} proteins. (B) Double labeling with the N-terminal Chromator mAb 12H9 (red) and Hoechst 33258 (blue) of polytene squashes from a *Chro*^{71}/*Chro*^{612} female third-instar larvae. The composite image (comp) is shown to the left. (C) Labeling with the JIL-1 pAb Hope of polytene squashes from wild-type (left micrograph) and *Chro*^{71}/*Chro*^{612} (right micrograph) male third-instar larvae. Note the upregulation of JIL-1 on the male X chromosome (X) of both wild-type and *Chro*^{71}/*Chro*^{612} mutant larvae.

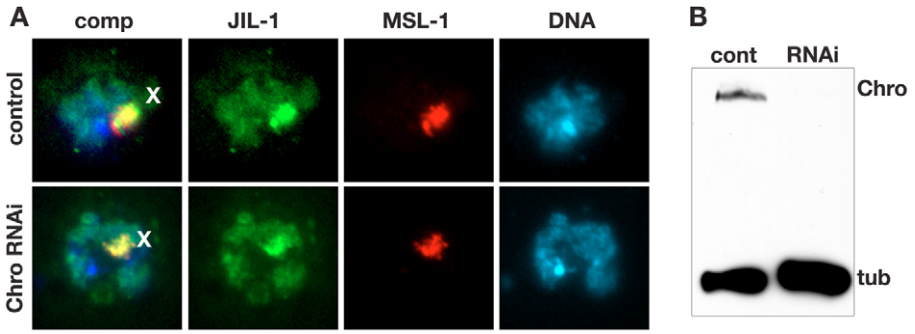

Fig. 7. RNAi depletion of Chromator in S2 cells does not affect JIL-1 chromosome localization. (A) Triple labelings with the JIL-1 pAb Hope (green), anti-MSL-1 antibody (red) and Hoechst 33258 (blue) of Chromator dsRNA treated S2 cells (lower panel) and mock-treated control cells (upper panel). The composite image (comp) is shown to the left and the location of the X chromosome is indicated with an X. (B) Western blot with Chromator mAb 6H11 of control-treated and Chromator RNAi-treated S2 cells from the cultures shown in A. In the RNAi sample Chromator protein levels (Chro) was substantially reduced compared with the level observed in the control cells. Tubulin levels (tub) are shown as a loading control.

Chro and *JIL-1* by generating double-mutant individuals. Since *Chro* and *JIL-1* both are located on the third chromosome we first recombined each of the $Chro^{71}$ *and* $Chro^{612}$ alleles onto the $JIL\text{-}1^{z2}$ chromosome. Subsequently, $JIL\text{-}1^{z2}$ $Chro^{71}$*/TM6 Sb Tb* males were crossed with $JIL\text{-}1^{z2}$ $Chro^{612}$*/TM6 Sb Tb* virgin females generating $JIL\text{-}1^{z2}$ $Chro^{71}/JIL\text{-}1^{z2}$ $Chro^{612}$ progeny. In control experiments we crossed $JIL\text{-}1^{z2}$*/TM6 Sb Tb* males with $JIL\text{-}1^{z2}$*/TM6 Sb Tb* virgin females generating $JIL\text{-}1^{z2}/JIL\text{-}1^{z2}$ progeny as well as $Chro^{71}$*/TM6 Sb Tb* males with $Chro^{612}$*/TM6 Sb Tb* virgin females generating $Chro^{71}/Chro^{612}$ progeny. In these crosses the *TM6* chromosome was identified by the *Tb* marker. Consequently, the experimental genotypes could be distinguished from balanced heterozygotic larvae by being non-*Tb* and the expected mendelian ratio of non-*Tb* to *Tb* larvae would be 1:2 because *TM6/TM6* is embryonic lethal. Table 1 shows that individuals of both the $Chro^{71}/Chro^{612}$ and $JIL\text{-}1^{z2}/JIL\text{-}1^{z2}$ genotype develop into third-instar larvae in numbers that were not statistically different ($P>0.9$, χ^2-test) from the expected mendelian ratio with that of *TM6* balanced heterozygotes. However, in the $JIL\text{-}1^{z2}$ $Chro^{71}/JIL\text{-}1^{z2}$ $Chro^{612}$ double-mutant combination there was a clear statistically significant difference ($P<0.001$, χ^2-test) as no non-*Tb* third-instar larvae were observed. This suggests that a simultaneous reduction in both JIL-1 and Chromator function synergistically reduces viability during development and is consistent with the hypothesis that the two proteins interact in vivo.

Discussion

In this study we have generated two new hypomorphic *Chro* alleles and analyzed the consequences of reduced Chromator protein function on polytene chromosome structure. We show that in $Chro^{71}/Chro^{612}$ mutants the polytene chromosome arms were coiled and compacted with a misalignment of band and interband regions and with numerous ectopic contacts connecting non-homologous regions. Furthermore, we demonstrate that Chromator co-localizes with JIL-1 at polytene interband regions and that the two proteins interact within the same protein complex. Overlay assays and deletion construct analysis suggested that the interaction between JIL-1 and Chromator is direct and that it is mediated by sequences in the C-terminal domain of Chromator and by the acidic region within the C-terminal domain of JIL-1. However, studies in S2 cells with RNAi-mediated Chromator depletion and in $JIL\text{-}1^{z2}$ homozygous null mutant backgrounds demonstrated that neither protein is likely to be dependent on the other for its chromatin localization. This suggests that other member(s) of the complex serving as chromatin-targeting factors remain to be discovered or that both proteins may have the ability to directly bind to DNA.

Although the *Drosophila* polytene chromosome has served as a widely used model for studying chromatin structure, remarkably little is known about its spatial organization or about the molecular basis for the conjugation of homologous

Table 1. Genetic interaction between *JIL-1* and *Chro* alleles

Cross	Genotypes: Number of third instar larvae		% Expected ratio*
$JIL\text{-}1^{z2}$ $Chro^{71}$*/TM6* × $JIL\text{-}1^{z2}$ $Chro^{612}$*/TM6*	$JIL\text{-}1^{z2}$ $Chro^{71}/JIL\text{-}1^{z2}$ $Chro^{612}$	$JIL\text{-}1^{z2}$ $Chro^{71}$*/TM6* or $JIL\text{-}1^{z2}$ $Chro^{612}$*/TM6*	
	0	664	0.0%
$Chro^{71}$*/TM6* × $Chro^{612}$*/TM6*	$Chro^{71}/Chro^{612}$	$Chro^{71}$*/TM6* or $Chro^{612}$*/TM6*	
	271	601	93.2%
$JIL\text{-}1^{z2}$*/TM6* × $JIL\text{-}1^{z2}$*/TM6*	$JIL\text{-}1^{z2}/JIL\text{-}1^{z2}$	$JIL\text{-}1^{z2}$*/TM6*	
	147	320	94.4%

*In these crosses the *TM6* chromosome was identified by the *Tubby* marker. Consequently, the experimental genotypes could be distinguished from balanced heterozygotic larvae by absence of the *Tubby* marker. The expected mendelian ratio of non-*Tubby* to *Tubby* larvae was 1:2 because *TM6/TM6* is embryonic lethal. The percentage of expected genotypic ratios were calculated as: observed non-*Tubby* larvae × 300/total observed larvae.

chromatids in the process of polytenization (Ananiev and Barsky, 1985; Schwartz et al., 2001). Recently it has been demonstrated that JIL-1 kinase, which phosphorylates histone H3 Ser10 in interband regions, plays a crucial role in maintaining polytene chromosome structure (Wang et al., 2001; Deng et al., 2005; Zhang et al., 2006). In the absence of JIL-1 there is a shortening and folding of the chromosomes with a non-orderly intermixing of euchromatin and the compacted chromatin characteristic of banded regions (Deng et al., 2005) and there is a striking redistribution of the heterochromatin markers dimethyl H3K9 and HP1 to ectopic chromosome sites (Zhang et al., 2006). This suggested a model where JIL-1 kinase activity functions to maintain chromosome structure and euchromatic regions by counteracting heterochromatization mediated by histone H3 dimethylation and HP1 recruitment (Zhang et al., 2006). However, the *Chro* mutant analysis presented here suggests that JIL-1 activity is necessary but not sufficient for maintaining some of these aspects of polytene chromosome morphology and that Chromator function is also required. Nonetheless, it should be noted that although the polytene chromosome phenotypes of *JIL-1* and *Chro* mutants resemble each other with coiled and compacted chromosome arms they are not identical. In contrast to *JIL-1* mutant polytene chromosomes, in *Chro* mutants there is still a clear demarcation between band and interband regions at the ultrastructural level although these bands are severely misaligned. Furthermore, in *JIL-1* null mutants the male X chromosome is differentially affected with a 'puffed' appearance whereas in *Chro* mutants the morphology of the male X chromosome is similar to that of the autosomes. Thus, it is likely that JIL-1 and Chromator control different but related aspects of chromosome morphology within the complex. That both proteins are necessary and may function synergistically is supported by the finding that a concomitant reduction in JIL-1 and Chromator function dramatically reduces viability during development.

An important feature of the Chromator protein is the presence of a chromodomain. The function of most chromodomain proteins identified thus far has been related to the establishment or maintenance of a variety of chromatin conformations (Cavalli and Paro, 1998; Brehm et al., 2004). For example, HP1 binds to methylated histone H3 and is essential for the assembly of heterochromatin (Nielsen et al., 2001; Jacobs and Khorasanizadeh, 2002; Peters et al., 2001). Thus, it is possible that Chromator through interactions mediated by its chromodomain participates in a complex with JIL-1 that is required for maintaining properly separated and aligned interband regions as well as a more open chromatin configuration. However, loss of JIL-1 or Chromator function also influences the coherence and organization of bands although neither protein is present in these regions. This suggests that JIL-1 and Chromator function may affect the distribution and/or activity of other molecules important for influencing chromatin structure such as boundary elements and/or the molecular machinery regulating heterochromatin formation and spreading. In support of this notion it has recently been demonstrated that the lethality as well as some of the chromosome morphology defects observed in *JIL-1* null or hypomorphic mutant backgrounds may be the result of ectopic histone methyltransferase activity (Zhang et al., 2006).

In addition to the present studies demonstrating an interaction with JIL-1, Chromator has been shown to interact with the spindle matrix protein skeletor (Walker et al., 2000; Rath et al., 2004) and with the zinc-finger protein Z4 (Eggert et al., 2004; Gortchakov et al., 2005). The interaction with skeletor was first detected in a yeast two-hybrid screen and subsequently confirmed by pull-down assays (Rath et al., 2004). Immunocytochemical labeling of *Drosophila* embryos, S2 cells and polytene chromosomes demonstrated that the two proteins show extensive co-localization during the cell cycle although their distributions are not identical (Rath et al., 2004). During interphase Chromator is localized on chromosomes to interband chromatin regions in a pattern that overlaps that of skeletor. During mitosis both Chromator and skeletor detach from the chromosomes and align together in a spindle-like structure with Chromator additionally being localized to centrosomes that are devoid of skeletor-antibody labeling. The extensive co-localization of the two proteins is compatible with a direct physical interaction between skeletor and Chromator. However, at present it is not known whether such an interaction occurs throughout the cell cycle or is present only at certain stages with additional proteins mediating complex assembly at other stages. The interaction of Chromator with Z4 was identified in co-immunoprecipitation experiments and the two proteins colocalize extensively at interband polytene regions (Eggert et al., 2004). However, Chromator and Z4 do not appear to associate directly and their chromosomal binding is independent of each other (Gorthakov et al., 2005). Interestingly, the phenotype of loss of Z4 function is somewhat different from that of loss of JIL-1 or Chromator function. *Z4* mutant chromosomes decompact and attain a cloudy appearance when losing their band/interband organization (Eggert et al., 2004) instead of coiling and shortening as in *JIL-1* and *Chro* loss-of-function mutants. This differential effect on polytene chromosome banding patterns and morphology may reflect that these constituents contribute different activities within one complex or may indicate the presence of more than one molecular assembly, each with different functions. Thus, future studies will be necessary to clarify the interactions of Chromator with interband-specific proteins and its functional role in establishing or maintaining polytene chromosome structure.

Materials and Methods

Drosophila stocks and generation of new *Chro* alleles

Fly stocks were maintained according to standard protocols (Roberts, 1998). Canton-S was used for wild-type preparations. The lethal *Chro* P-element insertion allele *KG03258* is described in Rath et al. (Rath et al., 2004) and the $JIL\text{-}1^{z2}$ null allele is described in Wang et al. (Wang et al., 2001) and in Zhang et al. (Zhang et al., 2003). New *Chro* mutant alleles were generated by ethyl methyl sulfonate (EMS) mutagenesis using standard procedures (Grigliatti, 1986). In this screen w^{1118} males that had wild-type alleles of *Chro* were treated with 25 mM EMS in a 1% sucrose solution for 18-20 hours. EMS-treated males were then mass mated with w^{1118} *TM2 Ubx e/TM6 Sb Tb e* virgin females. Male w^{1118}*/Y;*/TM6 Sb Tb e* progeny from these mass matings were selected and individually mated with *y* w^{1118} *KG03258/TM6 Sb Tb e* virgin females. The progeny of these single male matings were screened for potential new *Chro* alleles that reduced adult survival rates by more than 50% when heterozygous with the *KG03258* allele. Twelve such new *Chro* alleles were identified in this screen and outcrossed for six generations to w^{1118} *TM2 Ubx e/TM6 Sb Tb e* flies to eliminate non-specific second-site mutations on the other chromosomes. Complementation tests between the newly generated alleles revealed that individuals heteroallelic for two of these alleles, $Chro^{71}$ and $Chro^{612}$, survive to third-instar larval stages. The molecular lesions of $Chro^{71}$ and $Chro^{612}$ were determined by PCR mapping and sequencing as described (Zhang et al., 2003). Recombinant $JIL\text{-}1^{z2}$ $Chro^{71}$ and $JIL\text{-}1^{z2}$ $Chro^{612}$ chromosomes were generated by standard crosses as described (Ji et al., 2005) and the genotypes confirmed by PCR analysis (Zhang et al., 2003). Balancer chromosomes and markers are described (Lindsley and Zimm, 1992).

Antibodies

The Chromator-specific mAbs 6H11 and 12H9 have been previously characterized (Rath et al., 2004) and the anti-MSL-1 rabbit antiserum was the generous gift of M. Kuroda (Harvard Medical School, Boston, MA) and R. Kelley (Baylor College of Medicine, Houston, TX). The affinity-purified Hope rabbit anti-JIL-1 polyclonal antibody was described in Jin et al. (Jin et al., 1999) and the anti-GST mAb 8C7 in Rath et al. (Rath et al., 2004). The anti-α-tubulin and anti-V5 antibodies were obtained from commercial sources (Sigma-Aldrich and Invitrogen, respectively).

Immunohistochemistry and ultrastructural analysis

Polytene chromosome squash preparations were performed as in Kelley et al. (Kelley et al., 1999) using the 5 minute fixation protocol and labeled with antibody as described (Jin et al., 1999). S2 cells were affixed onto poly-L-lysine coated coverslips and fixed with Bouin's fluid for 10 minutes at 24°C and methanol for 5 minutes at –20°C. The cells on the coverslips were permeabilized with PBS containing 0.5% Triton X-100 and incubated with diluted primary antibody in PBS containing 0.1% Triton X-100, 0.1% sodium azide and 1% normal goat serum for 1.5 hour. Double and triple labelings using epifluorescence were performed using various combinations of antibodies and Hoechst 33258 to visualize the DNA. The appropriate species- and isotype-specific Texas Red-, TRITC- and FITC-conjugated secondary antibodies (Cappel/ICN, Southern Biotech) were used (1:200 dilution) to visualize primary antibody labeling. The final preparations were mounted in 90% glycerol containing 0.5% *n*-propyl gallate. The preparations were examined using epifluorescence optics on a Zeiss Axioskop microscope and images were captured and digitized using a high-resolution Spot CCD camera. Confocal microscopy was performed with a Leica confocal TCS NT microscope system equipped with separate Argon-UV, Argon, and Krypton lasers and the appropriate filter sets for Hoechst, FITC, Texas Red and TRITC imaging. A separate series of confocal images for each fluorophor of double-labeled preparations were obtained simultaneously with *z*-intervals of typically 0.5 μm using a PL APO 100×/1.40-0.70 oil objective. Images were imported into Photoshop where they were pseudocoloured, image processed and merged. In some images non-linear adjustments were made for optimal visualization of Hoechst labeling of chromosomes. For ultrastructural studies we prepared polytene chromosome squash preparations of wild-type and $Chro^{71}/Chro^{612}$ third-instar larvae according to the procedure of Semeshin et al. (Semeshin et al., 2004) as described in Deng et al. (Deng et al., 2005).

SDS-PAGE and immunoblotting

SDS-PAGE was performed according to standard procedures (Laemmli, 1970). Electroblot transfer was performed as described (Towbin et al., 1979) with transfer buffer containing 20% methanol and in most cases including 0.04% SDS. For these experiments we used the Bio-Rad Mini PROTEAN II system, electroblotting to 0.2 μm nitrocellulose and using anti-mouse HRP-conjugated secondary antibody (Bio-Rad) (1:3000) for visualization of primary antibody diluted 1:1000 in Blotto. The signal was visualized using chemiluminescent detection methods (SuperSignal kit, Pierce). The immunoblots were digitized using a flatbed scanner (Epson Expression 1680). Immunoblot analysis of $Chro^{71}/Chro^{612}$ mutants was performed as described (Wang et al., 2001; Zhang et al., 2003) using extracts from third-instar larvae with wild-type larvae as controls.

Overlay experiments

The four truncated GST-JIL-1 fusion proteins, JIL-1-NTD (residues 1-211), JIL-1-KDI (residues 251-554), JIL-1-KDII (residues 615-917) and JIL-1-CTD (residues 927-1207) have been previously described (Jin et al., 2000) and the constructs JIL-1-CTD-A (residues 887-1033) and JIL-1-CTD-B (residues 1034-1207) were described in Bao et al. (Bao et al., 2005). Two Chromator GST-fusion proteins, Chro-NTD (residues 1-346) and Chro-CTD (residues 329- 926) were cloned into the pGEX4T vector using standard techniques (Sambrook and Russell, 2001). The respective GST-fusion proteins were expressed in XL1-Blue cells (Stratagene) and purified over a glutathione agarose column (Sigma-Aldrich) according to the pGEX manufacturer's instructions (Amersham Pharmacia Biotech). For the overlay interaction assays approximately 2 μg GST or of the appropriate JIL-1 GST-fusion proteins were fractionated by SDS-PAGE and electroblotted to nitrocellulose. The blots were subsequently incubated with approximately 2 μg of either the Chro-NTD or the Chro-CTD GST-fusion protein overnight at 4°C in PBS with 0.5% Tween-20 on a rotating wheel. The blots were washed four times for 10 minutes each in PBS with 0.5% Tween-20 and binding detected by antibody labeling with either Chromator mAb 6H11 or 12H9. Input proteins were analyzed by SDS-PAGE and immunoblotting with GST-antibody.

Immunoprecipitation assays

For co-immunoprecipitation experiments, anti-JIL-1 or anti-Chromator antibodies were coupled to protein-A beads (Sigma) as follows: 10 μl of affinity-purified Hope anti-JIL-1 serum or 10 μl mAb 6H11 was coupled to 30 μl protein-A-Sepharose beads (Sigma) for 2.5 hours at 4°C on a rotating wheel in 50 μl IP buffer (20 mM Tris-HCl pH 8.0, 10 mM EDTA, 1 mM EGTA, 150 mM NaCl, 0.1% Triton X-100, 0.1% Nonidet P-40, 1 mM Phenylmethylsulfonyl fluoride and 1.5 μg aprotinin). The appropriate antibody-coupled beads or beads only were incubated overnight at 4°C with 200 μl S2 cell lysate on a rotating wheel. Beads were washed three times for 10 minutes each with 1 ml IP buffer with low-speed pelleting of beads between washes. The resulting bead-bound immunocomplexes were analyzed by SDS-PAGE and western blotting according to standard techniques (Harlow and Lane, 1988) using mAb 6H11 to detect Chromator and Hope antiserum to detect JIL-1. For V5-antibody immunoprecipitation experiments in S2 cells we used a full-length Chromator (926 aa) construct with an in-frame V5 tag at the C-terminal end previously described by Rath et al. (Rath et al., 2004). The S2 cells were transfected with this construct using a calcium phosphate transfection kit (Invitrogen) and expression was induced by 0.5 mM $CuSO_4$. Cells expressing the Chromator construct or mock-transfected control cells were harvested 18-24 hours after induction. Nuclear extracts were prepared as described (Smith et al., 2000), immunoprecipitated with 10 μl anti-V5 antibody coupled to 30 μl protein-A-Sepharose beads as described above, fractionated by SDS-PAGE, and immunoblotted using Hope JIL-1 antiserum for detection.

RNAi interference

dsRNAi in S2 cells was performed according to Clemens et al. (Clemens et al., 2000) and as described in Rath et al. (Rath et al., 2004). A 780 bp fragment encoding the 5′ end of Chromator cDNA was PCR amplified and used as templates for in vitro transcription using the Megascript™ RNAi kit (Ambion). 40 μg of synthesized dsRNA was added to 1×10^6 cells in six-well cell culture plates. Control dsRNAi experiments were performed identically except pBluescript vector sequence (800 bp) was used as a template. The dsRNA-treated S2 cells were incubated for 6-7 days and then processed for immunostaining and immunoblotting. For immunoblotting, 10^5 cells were harvested, resuspended in 50 μl S2 cell lysis buffer (50 mM Tris-HCl, pH 7.8, 150 mM NaCl and 1% Nonidet P-40), boiled and analyzed by SDS-PAGE and western blotting with anti-Chromator antibody (mAb 6H11) and anti-α-tubulin antibody.

We thank members of the laboratory for discussion, advice and critical reading of the manuscript. We also wish to acknowledge V. Lephart for maintenance of fly stocks and Laurence Woodruff for technical assistance. We especially thank M. Kuroda and R. Kelley for providing anti-MSL-1 antibody. This work was supported by NIH Grant GM62916 and NSF Grant MCB0445182 to K.M.J.

References

Ananiev, E. V. and Barsky, V. E. (1985). Elementary structures in polytene chromosomes of *Drosophila melanogaster*. *Chromosoma* **93**, 104-112.

Bao, X., Zhang, W., Krencik, R., Deng, H., Wang, Y., Girton, J., Johansen, J. and Johansen, K. M. (2005). The JIL-1 kinase interacts with lamin Dm_0 and regulates nuclear lamina morphology of *Drosophila* nurse cells. *J. Cell Sci.* **118**, 5079-5087.

Brehm, A., Tufteland, K. R., Aasland, R. and Becker, P. B. (2004). The many colours of chromodomains. *BioEssays* **26**, 133-140.

Cavalli, G. and Paro, R. (1998). Chromo-domain proteins: linking chromatin structure to epigenetic regulation. *Curr. Opin. Cell Biol.* **10**, 354-360.

Clemens, J. C., Worby, C. A., Simonson-Leff, N., Muda, M., Maehama, T., Hemmings, B. A. and Dixon, J. E. (2000). Use of double-stranded RNA interference in *Drosophila* cell lines to dissect signal transduction pathways. *Proc. Natl. Acad. Sci. USA* **97**, 6499-6503.

Deng, H., Zhang, W., Bao, X., Martin, J. N., Girton, J., Johansen, J. and Johansen, K. M. (2005). The JIL-1 kinase regulates the structure of *Drosophila* polytene chromosomes. *Chromosoma* **114**, 173-182.

Eggert, H., Gortchakov, A. and Saumweber, H. (2004). Identification of the *Drosophila* interband-specific protein Z4 as a DNA-binding zinc-finger protein determining chromosomal structure. *J. Cell Sci.* **117**, 4253-4264.

Gortchakov, A. A., Eggert, H., Gan, M., Mattow, J., Zhimulev, I. F. and Saumweber, H. (2005). Chriz, a chromodomain protein specific for the interbands of *Drosophila melanogaster* polytene chromosomes. *Chromosoma* **114**, 54-66.

Grigliatti, T. (1986). Mutagenesis. In *Drosophila: A Practical Approach* (ed. D. B. Roberts), pp. 39-58. Oxford: IRL Press.

Harlow, E. and Lane, E. (1988). *Antibodies: A Laboratory Manual*. 726 pp. Cold Spring Harbor, NY: Cold Spring Harbor Laboratory Press.

Jacobs, S. A. and Khorasanizadeh, S. (2002). Structure of HP1 chromodomain bound to a Lysine 9-methylated histone H3 tail. *Science* **295**, 2080-2083.

Ji, Y., Rath, U., Girton, J., Johansen, K. M. and Johansen, J. (2005). D-Hillarin, a novel W180-domain protein, affects cytokinesis through interaction with the septin family member Pnut. *J. Neurobiol.* **64**, 157-169.

Jin, Y., Wang, Y., Walker, D. L., Dong, H., Conley, C., Johansen, J. and Johansen, K. M. (1999). JIL-1: a novel chromosomal tandem kinase implicated in transcriptional regulation in *Drosophila*. *Mol. Cell* **4**, 129-135.

Jin, Y., Wang, Y., Johansen, J. and Johansen, K. M. (2000). JIL-1, a chromosomal kinase implicated in regulation of chromatin structure, associates with the MSL dosage compensation complex. *J. Cell Biol.* **149**, 1005-1010.

Kelley, R. L. and Kuroda, M. I. (1995). Equality for X chromosomes. *Science* **270**, 1607-1610.

Kelley, R. L., Meller, V. H., Gordadze, P. R., Roman, G., Davis, R. L. and Kuroda,

M. I. (1999). Epigenetic spreading of the *Drosophila* dosage compensation complex from *roX* RNA genes into flanking chromatin. *Cell* **98**, 513-522.

Kuroda, M. I., Kernan, M. J., Kreber, R., Ganetzky, B. and Baker, B. S. (1991). The maleless protein associates with the X chromosome to regulate dosage compensation in *Drosophila*. *Cell* **66**, 935-947.

Laemmli, U. K. (1970). Cleavage of structural proteins during assembly of the head of bacteriophage T4. *Nature* **227**, 680-685.

Lindsley, D. L. and Zimm, G. G. (1992). *The Genome of Drosophila melanogaster*. 1133 pp. New York: Academic Press.

Mortin, L. I. and Sedat, J. W. (1982). Structure of *Drosophila* polytene chromosomes. Evidence for a toroidal organization of the bands. *J. Cell Sci.* **57**, 73-113.

Nielsen, A. L., Oulad-Abdelghani, M., Ortiz, J. A., Remboutsika, E., Chambon, P. and Losson, R. (2001). Heterochromatin formation in mammalian cells: interaction between histones and HP1 proteins. *Mol. Cell* **7**, 729-739.

Peters, A. H., O'Carroll, D., Scherthan, H., Mechtler, K., Sauer, S., Schöfer, C., Weipoltshammer, K., Pagani, M., Lachner, M., Kohlmaier, A. et al. (2001). Loss of the Suv39h histone methyltransferase impairs mammalian heterochromatin and genome stability. *Cell* **107**, 323-327.

Rath, U., Wang, D., Ding, Y., Xu, Y.-Z., Qi, H., Blacketer, M. J., Girton, J., Johansen, J. and Johansen, K. M. (2004). Chromator, a novel and essential chromodomain protein interacts directly with the putative spindle matrix protein Skeletor. *J. Cell. Biochem.* **93**, 1033-1047.

Roberts, D. B. (ed.) (1998). *Drosophila: A Practical Approach*. 389 pp. Oxford: IRL Press.

Sambrook, J. and Russell, D. W. (2001). *Molecular Cloning: A Laboratory Manual*. Cold Spring Harbor, NY: Cold Spring Harbor Laboratory Press.

Schwartz, Y. B., Demakov, S. A. and Zhimulev, I. F. (2001). Polytene chromosome interband DNA is organized into nucleosomes. *Mol. Genet. Genomics* **265**, 311-315.

Semeshin, V. F., Belyaeva, E. S., Shloma, V. V. and Zhimulev, I. F. (2004). Electron microscopy of polytene chromosomes. *Methods Mol. Biol.* **247**, 305-324.

Smith, E. R., Pannuti, A., Gu, W., Steurnagel, A., Cook, R. G., Allis, C. D. and Lucchesi, J. C. (2000). The *Drosophila* MSL complex acetylates histone H4 at lysine 16, a chromatin modification linked to dosage compensation. *Mol. Cell. Biol.* **20**, 312-318.

Towbin, H., Staehelin, T. and Gordon, J. (1979). Electrophoretic transfer of proteins from polyacrylamide gels to nitrocellulose sheets: procedure and some applications. *Proc. Natl. Acad. Sci. USA* **9**, 4350-4354.

Walker, D. L., Wang, D., Jin, Y., Rath, U., Wang, Y., Johansen, J. and Johansen, K. M. (2000). Skeletor, a novel chromosomal protein that redistributes during mitosis provides evidence for the formation of a spindle matrix. *J. Cell Biol.* **151**, 1401-1411.

Wang, Y., Zhang, W., Jin, Y., Johansen, J. and Johansen, K. M. (2001). The JIL-1 tandem kinase mediates histone H3 phosphorylation and is required for maintenance of chromatin structure in *Drosophila*. *Cell* **105**, 433-443.

Zhang, W., Jin, Y., Ji, Y., Girton, J., Johansen, J. and Johansen, K. M. (2003). Genetic and phenotypic analysis of alleles of the *Drosophila* chromosomal JIL-1 kinase reveals a functional requirement at multiple developmental stages. *Genetics* **165**, 1341-1354.

Zhang, W., Deng, H., Bao, X., Lerach, S., Girton, J., Johansen, J. and Johansen, K. M. (2006). The JIL-1 histone H3S10 kinase regulates dimethyl H3K9 modifications and heterochromatic spreading in *Drosophila*. *Development* **133**, 229-235.

Zhimulev, I. F. (1996). Morphology and structure of polytene chromosomes. *Adv. Genet.* **34**, 1-497.

Zhimulev, I. F. and Belyaeva, E. S. (2003). Intercalary heterochromatin and genetic silencing. *BioEssays* **25**, 1040-1051.

Zhimulev, I. F., Belyaeva, E. S., Semeshin, V. F., Koryakov, D. E., Demakov, S. A., Demakova, O. V., Pokholkova, G. V. and Andreyeva, E. N. (2004). Polytene chromosomes: 70 years of genetic research. *Int. Rev. Cytol.* **241**, 203-275.

Journal of Cell Science